Chapter 3
Hydrodynamic Analysis of Tidal Inlets

3-1. Purpose and Scope

Inlets have been the focus of intense study by hydraulic engineers for many years (Watt 1905; Brown 1928; O'Brien 1931; Escoffier 1940, 1977; Bruun and Gerritsen 1960; Keulegan 1967; King 1974; Ozsoy 1977; Bruun 1978; van de Kreeke 1988). Hydraulic characteristics of interest to the practicing engineer consist of temporal and spatial variations of currents and water level in the inlet channel and vicinity. Depending on the degree of accuracy of the type of information needed, several predictive approaches are available. Although only approximate, relatively simple analytical procedures are commonly employed and yield quick answers. This chapter provides a brief description of inlet hydrodynamics and presents methods for performing an initial analysis of inlet stability and hydraulics. For more detailed descriptions of inlet hydraulics, physical and numerical modeling techniques are widely used (see Chapters 6 and 7, respectively).

3-2. Governing Equations

a. An idealized inlet system as shown in Figure 3-1 is considered to consist of a relatively short and narrow, but hydraulically wide, channel with mean depth h_c, cross-sectional area A_c, and length L_c. The sea tide represents the boundary condition, or forcing function, at one end of the channel and the bay at the other. The one-dimensional depth- and width-averaged shallow-water (long-wave) equation for the channel is

$$\frac{\partial u}{\partial t} + u\frac{\partial u}{\partial x} = -g\frac{\partial \eta}{\partial x} - g\frac{n^2 u|u|}{h_c^{4/3}} \tag{3-1}$$

where

$u(x,t)$ = cross-section averaged flow velocity along the channel length

t = time

$\eta(x,t)$ = tidal elevation with respect to mean water level

n = Manning's bed resistance coefficient

g = acceleration due to gravity

$n^2 u|u|/h_c^{4/3}$ = slope of the energy grade line in the channel

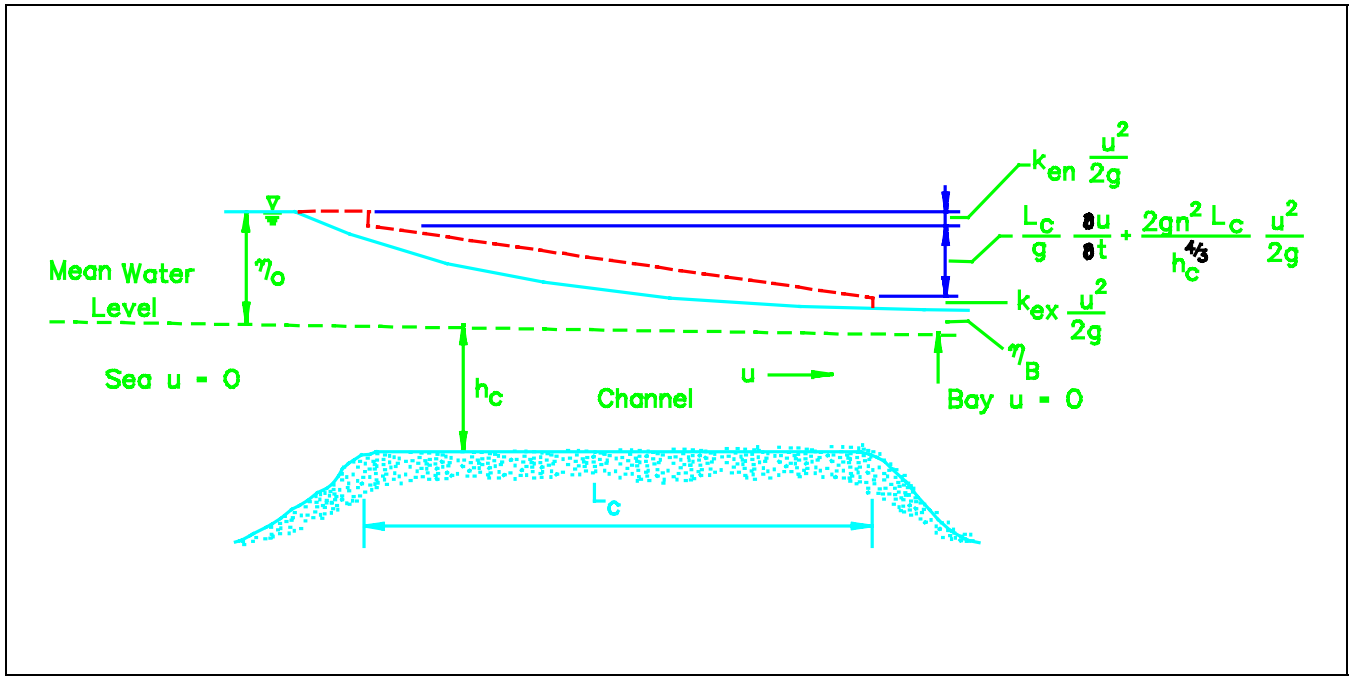

Figure 3-1. Idealized inlet channel showing contributions to head loss

With $\eta_o(t)$ and $\eta_B(t)$ representing tidal elevations in the sea and bay, respectively, integrating Equation 3-1 over length L_c gives

$$\eta_o - \eta_B = \frac{L_c}{g}\frac{\partial u}{\partial t} + \left(k_{en} + k_{ex} + \frac{2gn^2 L_c}{h_c^{4/3}} \right) \frac{u|u|}{2g} \tag{3-2}$$

where η and u are functions of time only. The quantities k_{en} and k_{ex} are the head loss coefficients associated with channel entrance and exit flows, respectively. The total head $\eta_o - \eta_B$ is the sum of four contributions: entrance loss, $k_{en}u^2/2g$; head loss due to bed friction, $2gn^2L_c/h_c^{4/3}$; head due to inertia, $(L_c/g)\partial u/\partial t$; and exit loss, $k_{ex}u^2/2g$ (Figure 3-1).

b. Assumptions associated with Equation 3-2 include a) bay and ocean current velocities are negligible compared to those in the channel, b) tidal amplitude is small compared to mean depth, and c) change in water volume in the channel due to tidal variation is negligible compared to mean volume in the channel.

c. To apply the momentum equation (Equation 3-2), a continuity expression for the bay storage volume S is needed. The discharge Q through an inlet is related to the rate of change of S and the rate of freshwater discharge Q_f from any upstream sources by $Q = Q_f + dS/dt$ where $Q = uA_c$, $S = \eta_B A_B$, and A_B is the surface area of the bay. Assuming that the tide propagates rapidly through the bay (i.e. the bay is relatively small and deep) so that spatial gradients in the water surface at any instant may be ignored, continuity may be described in terms of the velocity u as

$$u = \frac{A_B}{A_c}\frac{d\eta_B}{d_t} + \frac{Q_f}{A_c} \tag{3-3}$$

d. Additional simplifying assumptions are needed to solve Equations 3-2 and 3-3 analytically. First, it is assumed that the bay surface area and freshwater discharge are independent of time. Also, the ocean tide is considered to be sinusoidal, $\eta_o = a_o \sin(\sigma t - \tau)$ where a_o is the tidal amplitude, σ is tidal frequency, and τ is the angular measure of the lag of slack water in the channel after midtide in the ocean. Combining Equations 3-2 and 3-3 by eliminating u and substituting for η_o yields

$$\frac{d^2\eta_B}{dt^2} + \frac{FA_B}{2A_cL_c}\left(\frac{d\eta_B}{dt} + \frac{Q_f}{A_B}\right)\left|\frac{d\eta_B}{dt} + \frac{Q_f}{A_B}\right| + \frac{gA_c}{L_cA_B}\eta_B = \frac{gA_ca_o}{L_cA_B}\sin(\sigma t - \tau) \tag{3-4}$$

where $F = k_{en} + k_{ex} + 2gn^2L_c/h_c^{4/3}$. Since the quantity F represents the effect of all influences restricting flow, O'Brien and Clark (1974) referred to it as the overall impedance of the inlet.

e. Analytical solutions to Equations 3-3 and 3-4 that have appeared in the literature can be divided into two general groups: those in which both the freshwater inflow and the inertia term have been ignored and those in which the middle term on the left side of Equation 3-4 has been simplified (Brown 1928; Escoffier 1940; Keulegan 1951, 1967; van de Kreeke 1967; Mota Oliveira 1970; Dean 1971; Mehta and Ozsoy 1978). Although these solutions are of limited accuracy, they provide insight into the response of inlet-bay systems to tidal forcing and may be used as an order of magnitude check on more rigorous numerical solutions.

f. Keulegan's (1967) solutions are attractive because of their relative simplicity and are frequently incorporated in the derivation of inlet stability criteria. Assumptions include a) sinusoidal ocean tide, b) vertical inlet and bank walls, so that the water surface area remains constant, c) small tidal range compared to water depth, d) small time variation of water volume in the channel compared to mean channel volume, e) horizontal water surface of the bay, f) mean water level in the bay equal to that of the ocean, g) negligible flow acceleration in the channel, and h) no freshwater discharge. The head difference, therefore, is due to bed frictional dissipation, and entrance and exit losses and Equations 3-3 and 3-4 can then be solved for the channel current velocity and bay tide. Keulegan's results include the phase lag between bay and ocean tides and dimensionless values of bay amplitude. Both of these can be related to the dimensionless parameter K introduced by Keulegan as an expression for the hydraulic and geometric characteristics of an inlet and referred to as the coefficient of filling or repletion (Equation 3-5, Figure 3-2).

$$K = \left(\frac{T}{2\pi a_o}\right)\left(\frac{A_C}{A_B}\right)\left(2\frac{ga_o}{F}\right)^{1/2} \tag{3-5}$$

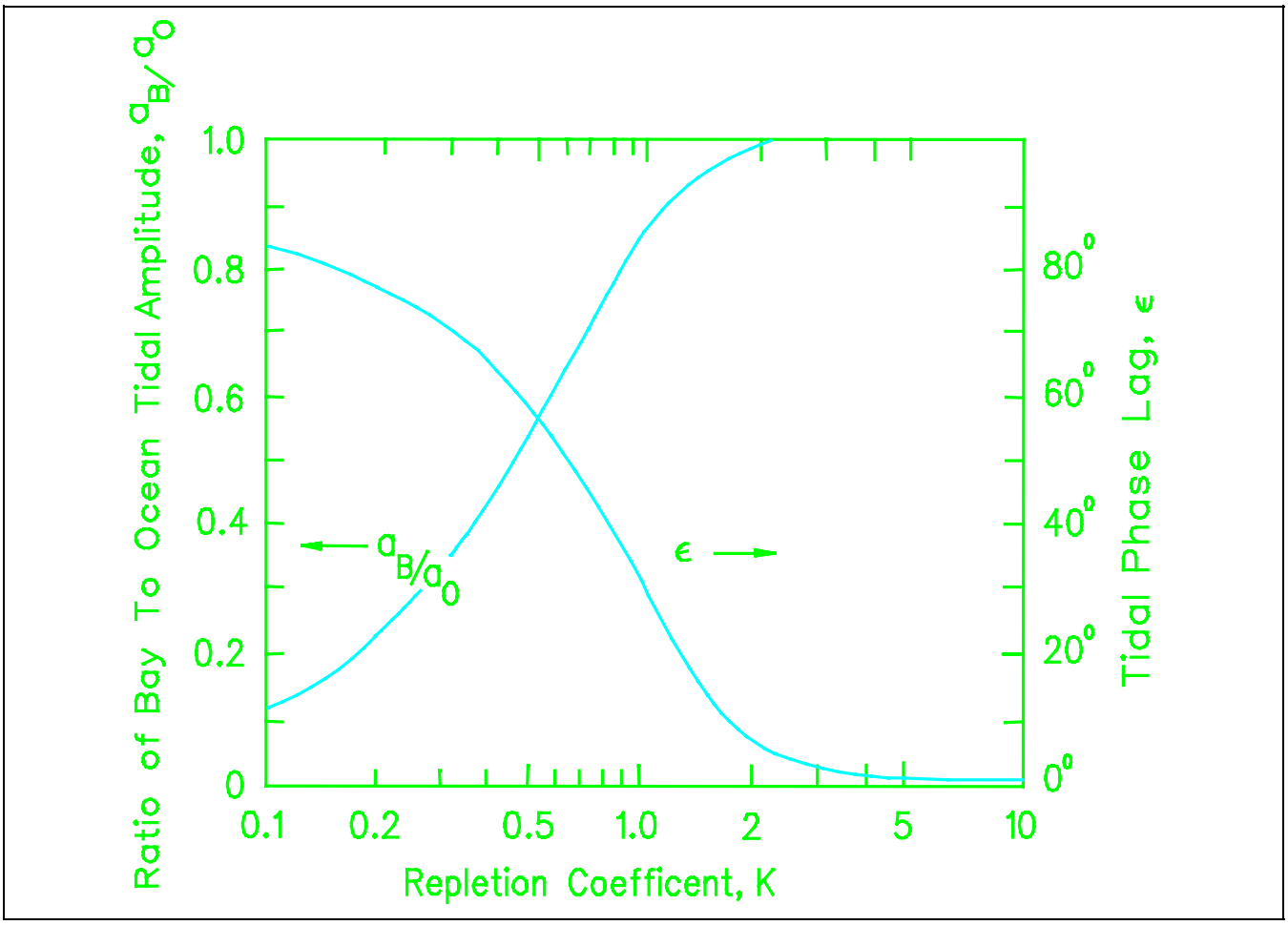

Figure 3-2. Relationship between the repletion coefficient and tidal phase lag and the ratio of bay to ocean tidal amplitude (after O'Brien and Dean (1972))

g. Keulegan also presented the relationship between K and dimensionless maximum velocity in the inlet V'_{max}[1] as shown in Figure 3-3. The maximum velocity V_{max} through a specific inlet is given by

$$V_{max} = V'_{max} \frac{2\pi}{T} a_o \frac{A_B}{A_c} \tag{3-6}$$

h. A set of tidal curves obtained by Keulegan's method is shown in Figure 3-4. Inherent in the result is that slack water corresponds to the time of maximum (and minimum) elevation in the bay. Maximum velocity occurs at midtide in the bay when $\eta_o - \eta_B$ is a maximum. Amplitudes increase with increasing values of the repletion coefficient. This is expected since K increases with increasing values of cross-sectional area, hydraulic radius, and decreasing values of energy loss and friction. Because of the absence of inertia, the bay tidal amplitude is never larger than the ocean tidal amplitude.

i. Another approach to solving Equations 3-3 and 3-4 has been presented by Mehta and Ozsoy (1978) and Walton and Escoffier (1981) where the inertia term is not dropped. In Mehta and Ozsoy's (1978) method, the system of equations themselves is not linearized; however, the generation of higher harmonics is neglected in obtaining a first-order solution. Assuming a sinusoidal variation in the flow velocity, results are obtained as shown in Figures 3-5 and 3-6. Dimensionless parameters incorporated in the solution are: bay amplitude $\hat{\alpha}_B = a_B/a_o$, channel velocity $\hat{\alpha}_m = u_m A_C/a_o \sigma A_B$, tidal frequency

[1] In presenting Keulegan's work, the symbol V is used to denote channel velocity because the V is carried over in the derivation of various stability criteria.

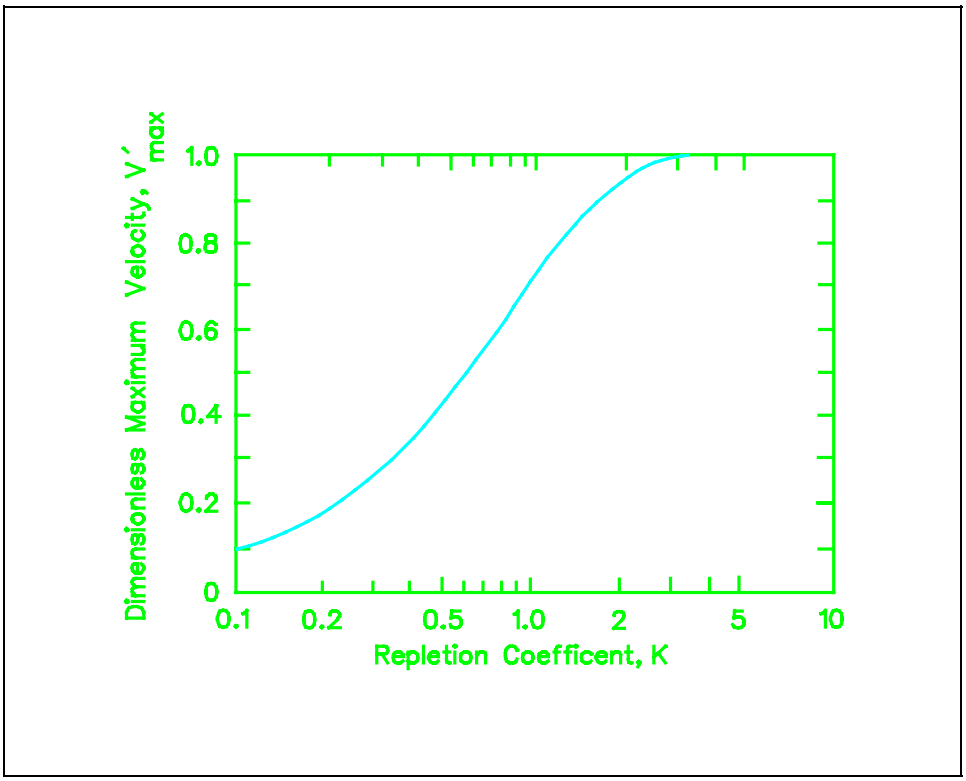

Figure 3-3. Relationship between repletion coefficient and dimensionless maximum velocity (after O'Brien and Dean (1972))

$\alpha = \sigma(L_C A_B / g A_C)^{1/2}$, and bed dissipation coefficient $\beta = -a_o F A_B / 2 L_C A_C$. Bay water level amplification is predicted under a certain range of α and β conditions and lag greater than 90 deg. Also, the time of slack water does not necessarily coincide with high or low tide in the bay; at slack, the bay and ocean tide elevations differ by an amount equal to the head from flow inertia. Results compare well with those obtained by King (1974).

3-3. Hydraulic Parameters

a. Ocean tidal amplitude. The ocean tidal amplitude a_o may be obtained from published National Ocean Service (NOS) tide tables or field measurements. To minimize influence from the inlet and any associated structures, gauges should be positioned away from areas directly affected by inlet currents and values obtained from tables should be interpolated from outer coast values on either side of the inlet (Mehta and Ozsoy 1978).

b. Equivalent length. The length of the idealized equivalent inlet channel L_c used in the preceding development is related to and may be obtained from the real length of the channel by requiring that the head loss due to bed friction be equal in the two cases. Escoffier (1977) introduced the hypothetical quantity L_c, the equivalent length of a channel, as

$$L_c = A_c^2 \, h_c^{4/3} \sum_{i=1}^{i=m} \frac{\Delta x_i}{h_i^{4/3} A_i^2} \tag{3-7}$$

In using the equation, the real inlet channel is divided into m sections of lengths Δx_i. Each section is chosen of such a length that over this length, the cross-sectional area A_i and mean depth h_i may be assumed constant. A basic assumption in deriving Equation 3-7 is that Manning's n is assumed to be independent of depth and is considered to characterize the channel bed roughness. O'Brien and Clark (1974) obtained a similar representation for L_c assuming the Darcy friction factor f to be constant rather than Manning's n. An equivalent channel cross-sectional area, rather than length, was used by Keulegan (1967).

c. Equivalent bay area. The condition of hydraulic bay filling is reasonably met only in relatively small bays

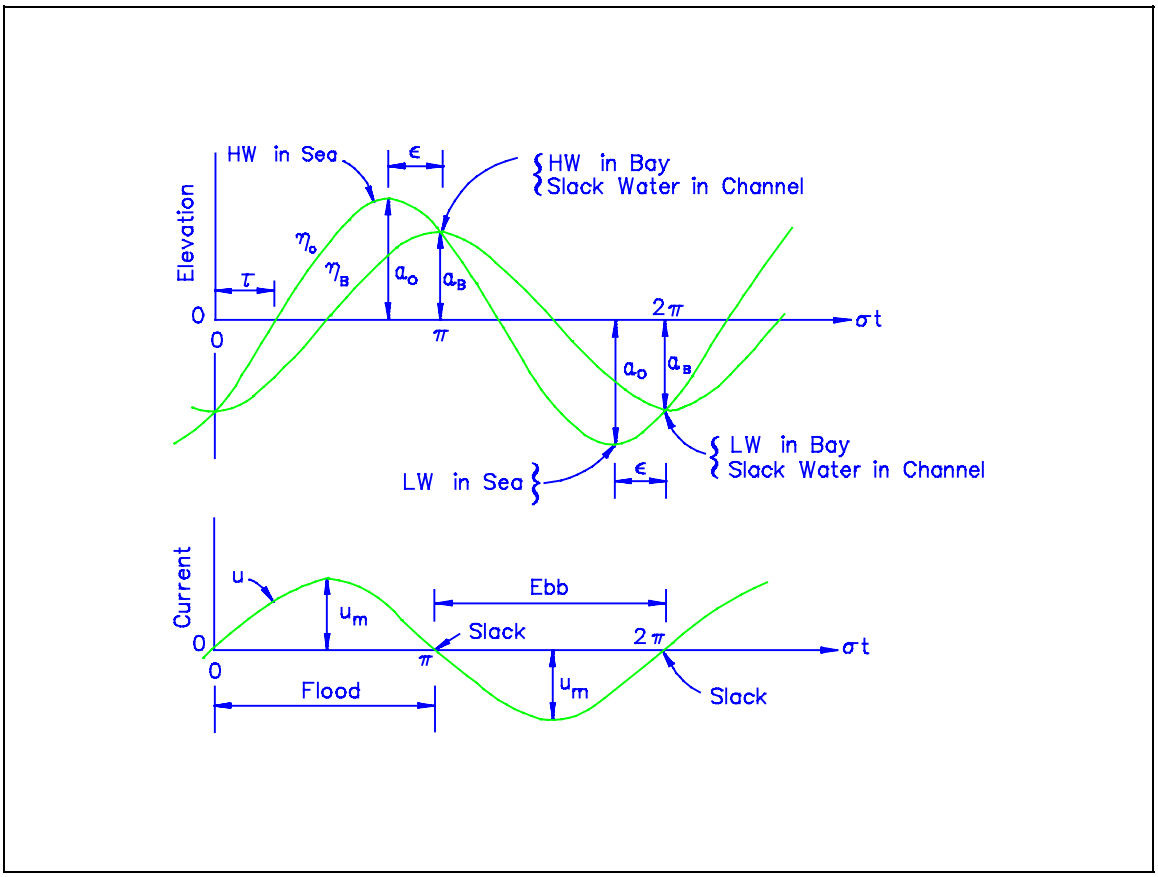

Figure 3-4. Ocean tide, bay tide, and current velocity through a channel as functions of dimensionless time (radians) (from Mehta and Joshi (1988))

(O'Brien and Clark 1974). Spatial water surface gradients due to inertia and bed friction in larger bays can be estimated using a simple approach involving the continuity principle (Escoffier 1977). If these gradients are not small compared to the bay tidal amplitude, Equation 3-3 is not applicable unless η_B is considered to be the tide at the bayward end of the inlet and A_B is redefined as an equivalent bay area corresponding to this tide. Equivalent bay area can be derived by dividing the tidal prism by the tidal range or by solving for it using Figure 3-5 and appropriate measurements of bay tidal amplitude a_B and a_o.

d. Bed resistance and loss coefficients.

(1) Bed resistance in an inlet channel varies with fluctuations in depth and bed form type that occur with changing tidal stage. For many engineering purposes, it is sufficient to estimate the bed resistance coefficient on a tide-averaged basis. Using the Chezy coefficient C (which is related to Manning's n according to $C = h_c^{1/6}/n$), Bruun and Gerritsen (1960) introduced an approximate empirical relationship: $C = \alpha_1 + \alpha_2 \log A_c$, based on measurements at sandy inlets with maximum velocities on the order of 1 m/sec (3.3 ft/sec). Proposed representative values of α_1 and α_2 were 30 $m^{1/2}$/sec and 5 $m^{1/2}$/sec, respectively, when A_c is in square meters and C is in $m^{1/2}$/sec (or α_1 = 44.3 $ft^{1/2}$/sec and α_2 = 9.4 $ft^{1/2}$/sec when A_c is in square feet and C is in $ft^{1/2}$/sec). In terms of Manning's n, the relationship between C and A_c can be written as

$$n = \frac{h_c^{1/6}}{\alpha_1 + \alpha_2 \log A_c} \tag{3-8}$$

********** EXAMPLE PROBLEM 3-1 **********

GIVEN: A bay with a surface area, A_B = 1.86 x 10^7 m^2 (2 x 10^8 ft^2) and an average depth of 6.1 m (20 ft) is located on the Atlantic coast. The tide is semidiurnal (T = 12.4 hr), with a spring range of 1.34 m (4.4 ft), as given by the National Ocean Survey Tide Tables (available from the National Oceanic and Atmospheric Administration). An inlet channel, which will be the only entrance to the bay, is to be constructed across the barrier beach which separates the bay from the ocean. The inlet is to provide a navigation passage for small vessels, dilution water to control bay salinity and pollution levels, and a channel for fish migration. The channel is to have a design length, L_c = 1,097 m (3,600 ft) with a pair of vertical sheet-pile jetties that will extend the full length of the channel. The channel has a depth below mean sea level (msl), h_c = 3.66 m (12 ft), and a width W_c = 183 m (600 ft).

FIND: The bay tidal range, maximum flow velocity V_{max}, and volume of water flowing into and out of the bay on a tidal cycle (tidal prism) for a tide having the spring range.

SOLUTION: Assume entrance and exit loss coefficients, k_{en} = 0.1, k_{ex} = 1.0, respectively, and n = 0.027.

$A_c = W_c\, h_c$ = (183 m)(3.66 m) = 669 m^2 (7,200 ft^2)

$F = k_{en} + k_{ex} + 2gn^2/(h_c^{4/3})$
$= 0.1 + 1.0 + (2)(9.81\ m/sec^2)(0.027)^2/(3.66\ m^{4/3})$
$= 3.88$

a_o = 1.34 m/2 = 0.67 m (2.2 ft)

Then by Equation 3-5,

$K = [(12.4\ hr)(3600\ sec/hr)/(2)(3.14)(0.67\ m)]\ [669\ m^2/(1.86 \times 10^7)]$
$[(2)(9.81\ m/sec^2)(0.67\ m)]^{1/2}\ /(3.88^{1/2})$
$= 0.7$

From Figures 3-2 and 3-3, with K = 0.7

V'_{max} = 0.58

and

a_b/a_o = 0.69, therefore

a_b = (0.69)(0.67 m) = 0.46 m (1.5 ft), and the bay tidal range is 2(0.46 m) = 0.92 m (3.0 ft)

From Equation 3-6, the maximum flow velocity is

$V_{max} = 0.58\ [(2)(3.14)/(12.4\ hr)(3600\ sec/hr)]\ (0.46\ m)$
$(1.86 \times 10^7\ m^2)/669\ m^2)$

$= 1.04$ m/sec (3.41 ft/sec)

The tidal prism is

$(2)(a_b)(A_b) = (2)(0.46\ m)(1.86 \times 10^7\ m^2) = 1.7 \times 10^7\ m^3$ (6.0 x 10^8 ft^3)

If the average depth of the bay is 6.1 m (20.0 ft) and the distance to the farthest point in the bay is 6.4 km (4.0 miles), the time t_* it will take for the tide wave to propagate to that point is

$t_* = L_b/[(g)(d_b)]^{1/2} = 6400\ m/[(9.81\ m/sec^2)\ (6.1\ m)]^{1/2}$
$= 827$ sec, or 0.23 hr

Since this time is significantly less than 12.4 hr, the assumption that the bay surface remains horizontal is quite satisfactory.

****

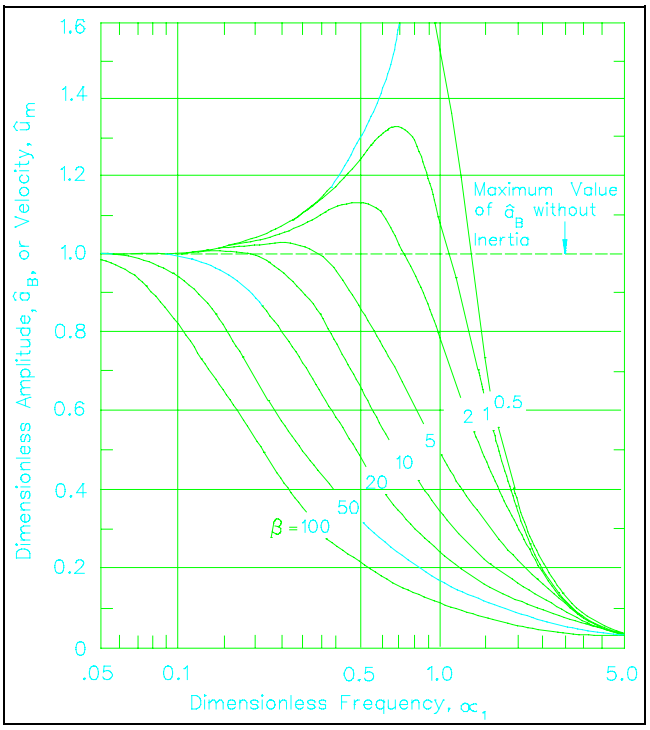

Figure 3-5. Dimensionless bay tidal amplitude or channel velocity as functions of dimensionless frequency (from Mehta and Ozsoy (1978))

Manning's n can be approximated using $A_c = h_c W_c$ and empirical relationships between throat depth and width in the form of $h_c = pW_c^q$, where p and q are coefficients, and W_c is the width at the inlet throat (Graham and Mehta 1981). For structured inlets, n ranges from 0.026 to 0.029, and from 0.025 to 0.027 for those without jetties (Mehta and Joshi 1988).

(2) Flow coming from a channel can be compared to that of a separated jet expanding from a narrow channel into a very large basin. Most of the energy dissipation occurs in the expanding part of the flow due to turbulence. Since the kinetic head is usually lost as the flow enters the basin, $k_{ex} = 1$. For flow entering a channel, energy loss is not very significant and $k_{en} \leq 0.05$.

e. Tidal current and prism.

(1) The tidal prism is the volume of water that is drawn into the bay, from the ocean and through the inlet, during flood tide. Aperiodicity of the tide, freshwater discharge, and the presence of other openings in the bay are some of the reasons why the prism in not always equal to the volume of water that leaves during the ebb. In the case of a single inlet-bay system with sinusoidal ocean tide, the tidal prism can be approximated by $2\,Q_m/\sigma C_K$ where $Q_m = u_m A_c$ is the maximum discharge and C_K is a parameter that varies with the repletion coefficient. The term C_K essentially accounts for the nonlinearity in the variation of discharge Q with time as a result of the quadratic head loss. At $K = 1$, $C_K = 0.81$ and at $K = 4$, $C_K = .999$ (Keulegan 1967). For simple calculations, an average value of 0.86 has been recommended by Keulegan and Hall (1950) and O'Brien and Clark (1974).

(2) For sandy inlets, the cross-sectional average velocity at the throat is on the order of 1 m/sec (3.3 ft/sec). For very small inlets, the velocity may be lower and for those with rocky bottoms, the velocity may be higher. To accurately determine the flow field, in situ measurements at several elevations across the flow section using current meters are recommended. It is important to keep in mind that typically well-defined ebb-and flood-dominated channels are present and flood flow is usually dominant near the bottom, while ebb flow is dominant near the surface.

3-4. Inlet Stability Criteria

a. Some inlets are permanent and remain open with relatively small changes in location, cross-sectional area, and shape; others are ephemeral or subject to intermittent openings and closings. The ability of an inlet to maintain itself in a state of stable equilibrium against wave activity and associated littoral transport depends on the availability of littoral material and the tidal prism. Many attempts at describing inlet stability have concentrated on empirical relationships between the tidal prism and inlet throat cross-sectional area (LeConte 1905; O'Brien 1931, 1969; Nayak 1971; Johnson 1973). Jarrett (1976) reviewed the previously established relationships and performed a regression analysis on data from 108 Pacific, Atlantic, and gulf coast inlets in various combinations in an attempt to determine best-fit equations. Results of his analysis indicated that the tidal prism-inlet (P) cross-sectional area (A) relationship is not a unique function for all inlets, but varies depending on inlet location and the presence or absence of jetties. Jarrett confirmed the original relationship established by O'Brien (1969) for inlets with two jetties

$$A = 4.69 \cdot 10^{-4}\, P^{0.85} \tag{3-9}$$

and concluded that natural inlets and single-jettied inlets on the three coasts exhibit slightly different P versus A

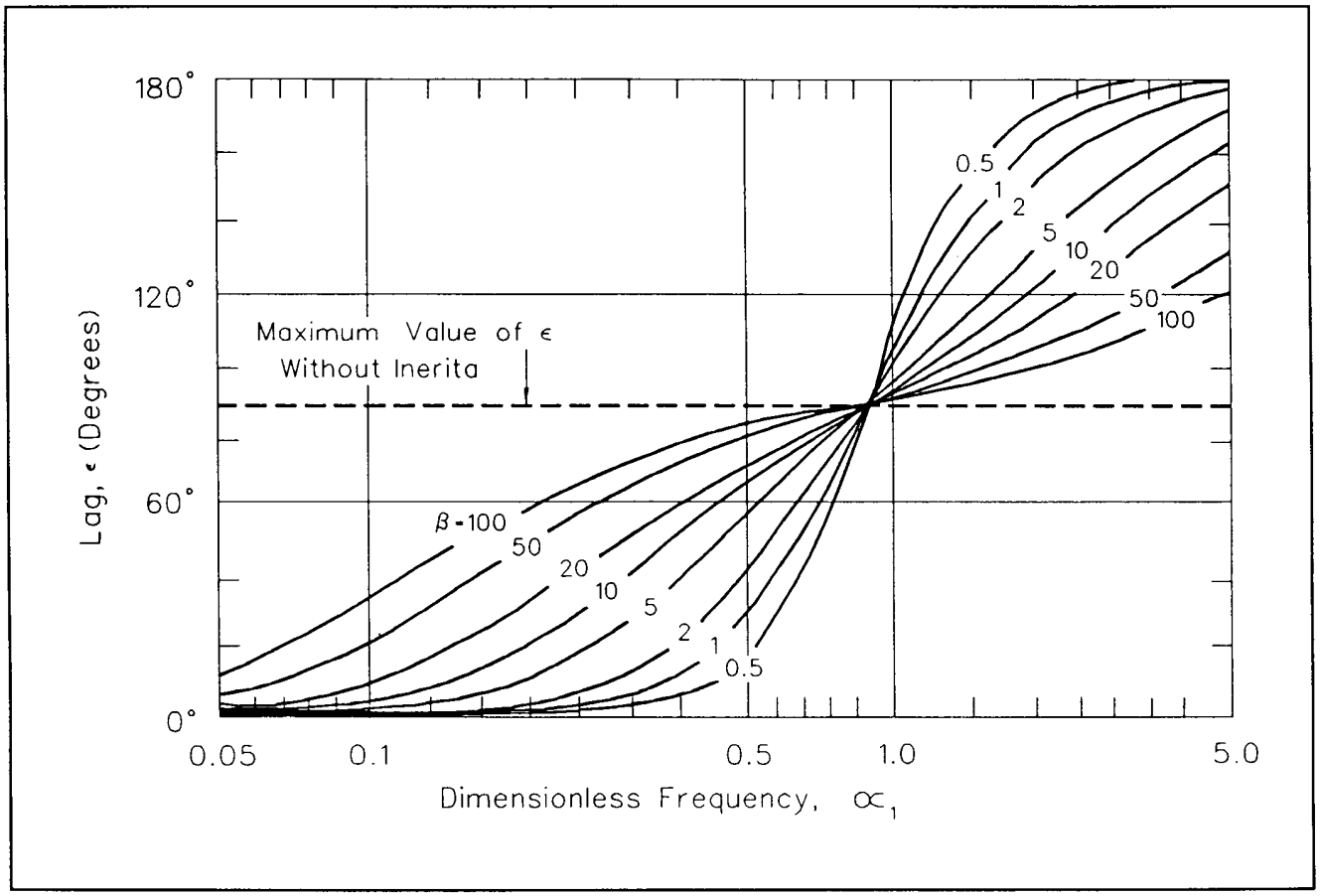

Figure 3-6. Lag as a function of dimensionless frequency (from Mehta and Ozsoy (1978))

relationships due to differences in tidal and wave characteristics (Figure 3-8).

b. The Ω/M criteria for inlet stability, where M is the total annual littoral drift, and Ω is the tidal prism, were introduced by Bruun and Gerritsen (1960) and elaborated on by Bruun (1978). The stability of an inlet is rated as good, fair, or poor according to the following:

$\Omega/M > 150$	Good
$100 \geq \Omega/M \leq 150$	Fair
$50 \geq \Omega/M \leq 100$	Fair to poor
$\Omega/M < 50$	Poor

c. Escoffier (1940) introduced a hydraulic stability curve, referred to as the Escoffier diagram, on which maximum velocity is plotted against cross-sectional flow area (Figure 3-9). A single hydraulic stability curve represents changing inlet conditions, when ocean tide parameters, and bay and inlet plan geometry conditions remain relatively fixed. If these conditions are drastically altered, a new stability curve is established. Each position on the curve represents a different value of Keulegan's repletion coefficient K, the ratio of bay to ocean tidal amplitude, and tidal phase lag between ocean high or low tide and slack water in the inlet.

********** EXAMPLE PROBLEM 3-2 **********

GIVEN: Information provided in Example 3-1.

FIND: Potential stability of the proposed channel cross section. Remember the channel has vertical sheet-pile walls, so its cross section can only change in the vertical.

SOLUTION: By varying the cross-sectional area of the channel A assuming that the channel width W_c remains constant and varying the channel depth h_c and recalculating the tidal prism as described in Example 3-1, the effect of channel area on the bay tidal prism can be evaluated and compared with Equation 3-9.

h_c (m)	0.91	1.8	2.4	4.9	7.6	10.7
K	0.11	0.29	0.44	1.1	2.0	2.7
V'_{max}	0.12	0.35	0.50	0.81	0.95	0.98
a_b/a_o	0.12	0.38	0.59	0.97	1.0	1.0
a_b	0.08	0.25	0.40	0.65	0.68	0.67
V_{max} (m/sec)	0.15	2.5	1.4	1.9	1.3	0.9
P $(x10^6)(m^3)$	3.0	9.3	14.9	24.2	25.3	24.9
A_c (m^2) $(=2a_bA_b)$	167.0	329.0	439.0	897.0	1,391.0	1,958.0
A_c (m^2) (Eqn 3-9)	150.0	393.0	587.0	886.0	920.0	908.0

Graphical results are presented in Figure 3-7. The common point on the two curves is the solution to the problem. In this case, however, two common points occur, indicating that the channel may either close at the lower point (approximately 220-m^2 (2,370-ft^2) cross-sectional area, and 1.2-m (4-ft^2) depth), or scour to the upper stability point (approximately 890-m^2 (9,600-ft^2) cross-sectional area, and 4.9-m (16-ft) depth). This indicates that the 183- by 3.7-m (600- by 12-ft) design channel would be unstable.

Where the hydraulic response curve lies above the stability curve, the tidal prism is too large for the inlet channel area and erosion will likely occur until a stable channel develops. If the hydraulic response curve crosses the stability curve twice, as in this example, the lower point is an unstable equilibrium point from which the channel can either close or scour to the upper stability point. If the hydraulic response curve is substantially below the stability curve at all points, a stable inlet channel is unlikely to develop and the channel should eventually close.

The stable inlet cross-sectional area depends on other factors (e.g., wave climate, monthly tidal range variations, surface runoff) besides the spring or diurnal tidal prism. As a result, the tidal prism - inlet area relationships (Figure 3-8) serve only as indications of the approximate stable cross-sectional area. The analysis performed in the example demonstrates that the design channel will most likely shoal or erode; however, the actual equilibrium depth will fluctuate with time, and can vary substantially from the indicated depths of 1.2 m (4 ft) or 4.9 m (16 ft).

****

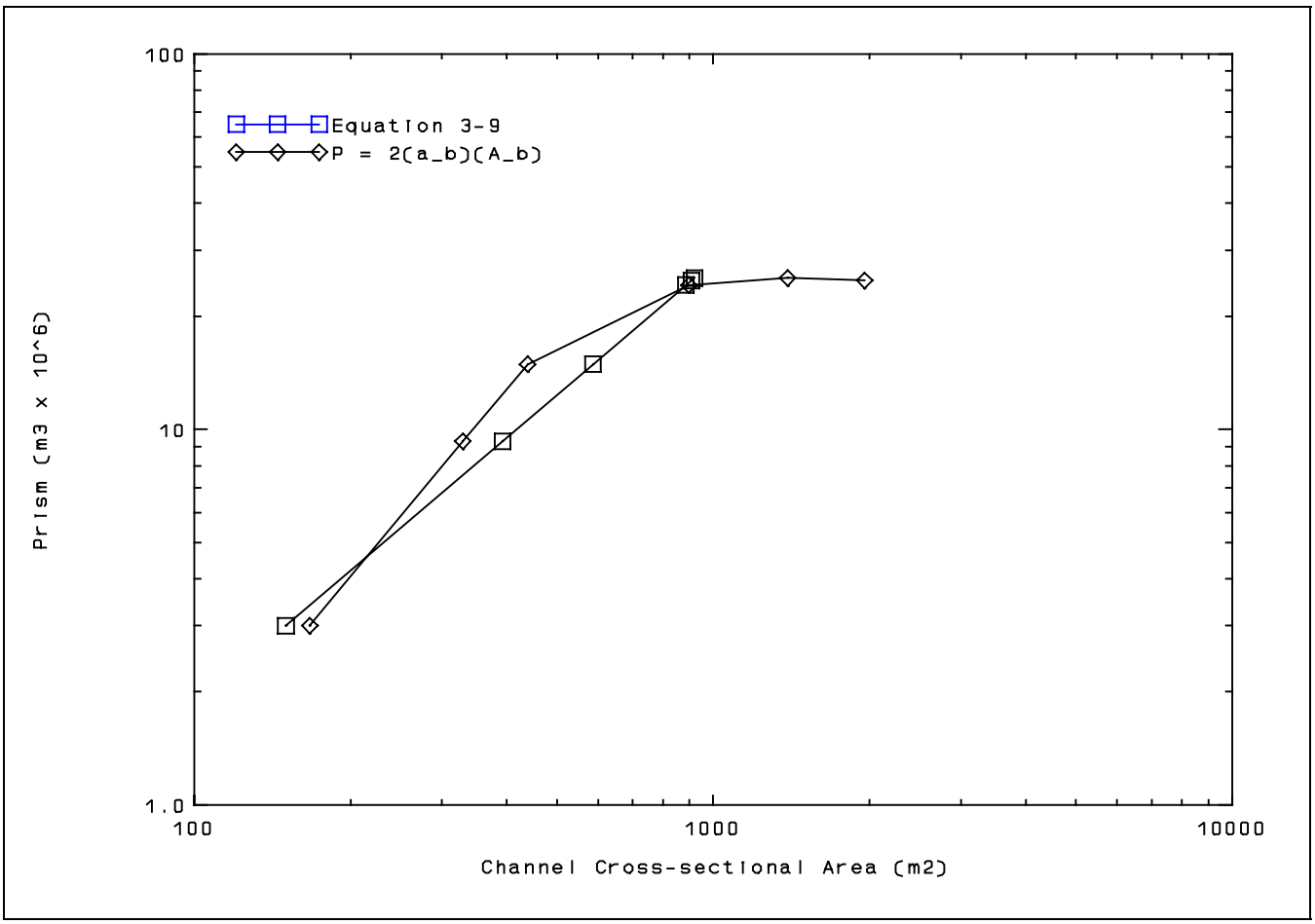

Figure 3-7. Graphical results for example problem 3-2

d. According to the Escoffier diagram, an inlet is hydraulically stable if its cross-sectional area is larger than the critical flow area A_{c*}. An induced change in the cross-sectional area of a stable inlet will result in a change in inlet velocity that attempts to return the inlet to its equilibrium size by appropriate deposition or scour. An inlet having a cross-sectional area smaller than the critical flow area is termed hydraulically unstable. The Escoffier diagram illustrates that any change in flow area is accompanied by a change in flow velocity that will perpetuate the induced change. Since any initial change in flow area is accentuated, the hydraulically unstable inlet will either continuously scour until the critical flow area is attained, or continuously shoal until inlet closure. Escoffier's hydraulic stability model has been applied in describing the behavior of "hydraulically stable" inlets by O'Brien and Dean (1972); Defenr and Sorensen (1973); and Mehta and Jones (1976).

e. In a later paper, Escoffier (1977), using Keulegan and O'Brien formulations, presented a variation of his original diagram that allows for the equilibrium value of V_{max} to vary with the repletion coefficient K. Dimensionless velocity values ν and ν_E (where $\nu = V_{max}/(2ga_o)^{1/2}$ and ν_E is the equilibrium value of ν), are plotted as functions of K (Figure 3-10). The letter A represents an unstable equilibrium point and B represents a stable equilibrium point. A small deviation from conditions represented by point A sets into operation forces that tend to reinforce that deviation. A similar deviation at B results in changes that tend to restore the inlet to its equilibrium point. Figure 3-11 shows several possible relative positions for the two curves. The first ν curve plots high enough to intersect the ν_E curve in two places, one stable and one unstable. The second ν curve has only one point of tangency with the ν_E curve, an unstable point. The third curve fails to reach the ν_E curve and therefore,

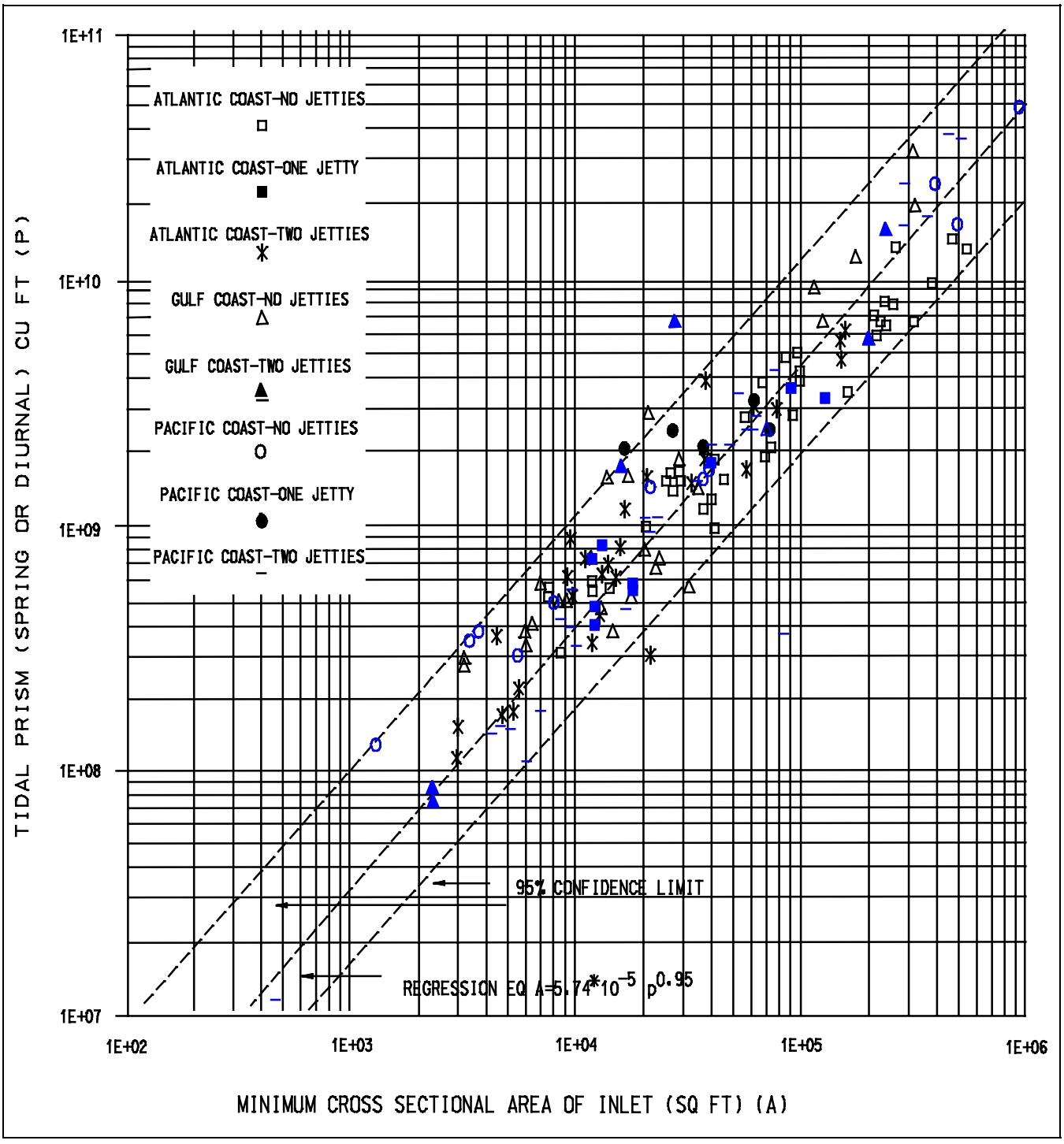

Figure 3-8. Tidal prism versus cross-sectional area for Pacific, Atlantic, and Gulf coast inlets (after Jarrett (1976))

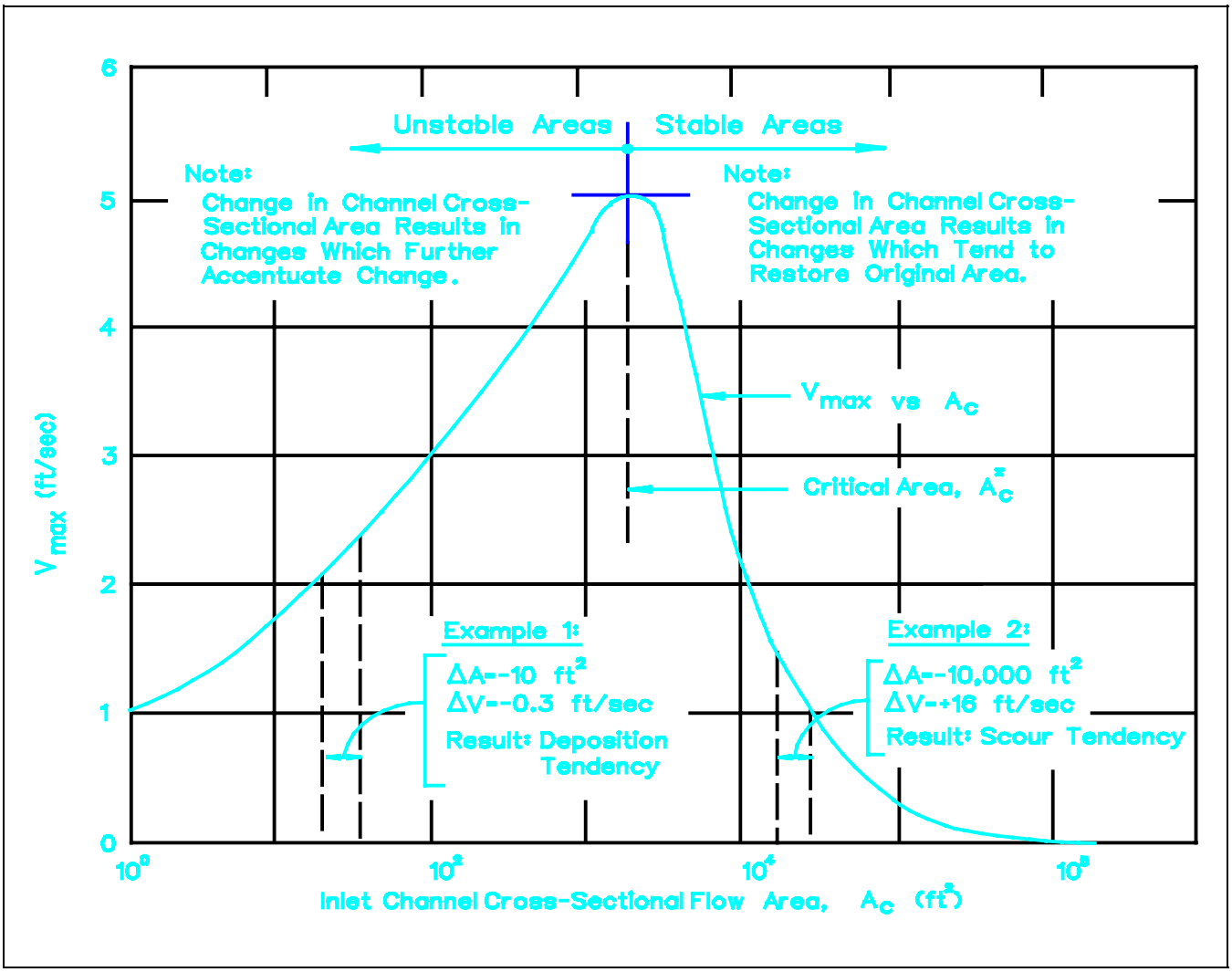

Figure 3-9. Generalization of Escoffier's hydraulic stability curve (after O'Brien and Dean (1972))

stability is not possible. Escoffier presented the idea of translating the height of the ν curve into a measure of stability, represented by the dimensionless parameter λ (Figure 3-12). The value of λ is equal to the ratio of ν to ν_E for the value of *K* that makes ν a maximum. The value of λ can be taken as a measure of the degree of stability; λ greater than 1 indicates stability.

f. O'Brien and Dean (1972) proposed a method of calculating the effect of deposition on stability of an inlet. Their method is based on earlier contributions by O'Brien (1931), Escoffier (1940), and Keulegan (1967), and assumes that a critical cross-sectional throat area A_{c*} exists with a corresponding critical velocity V_{max}. A stability index β represents the capacity of an inlet to resist closure under conditions of deposition. It incorporates the buffer storage area available in the inlet cross section, prior to deposition, and also includes the capability of the inlet to transport excess sand from its throat.

$$\beta = \int_{A_{C_*}}^{A_{CE}} (V_{max} - V_T)^3 \, dA_C \qquad (3\text{-}10)$$

where

β = stability index (units of length^5/time^3)

A_{CE} = cross-sectional area of throat

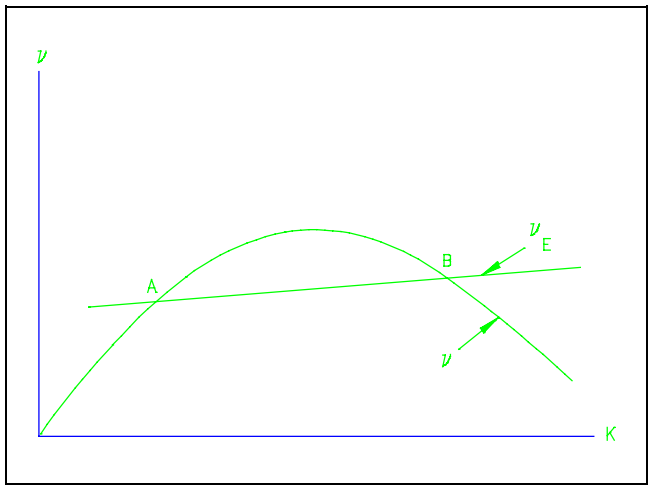

Figure 3-10. ν_E and ν versus repletion coefficient (from Escoffier (1977))

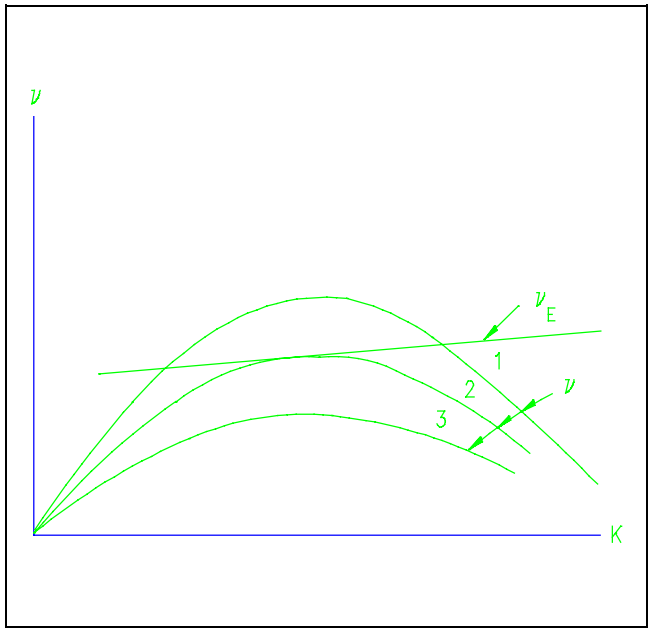

Figure 3-11. ν_E and various values of ν versus repletion coefficient (after Escoffier (1977))

V_{max} = maximum velocity in the throat

V_T = threshold velocity for sand transport

A_{C^*} = critical cross-sectional area (value of A_C at peak of V_{max} curve)

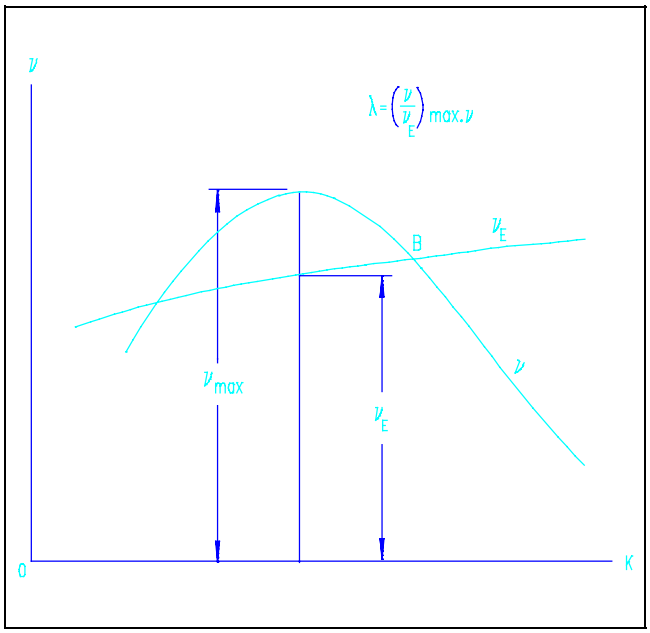

Figure 3-12. Definition diagram for the stability parameter λ (from Escoffier (1977))

Inlets with an equilibrium area much larger than the critical area have more storage area, and therefore, will be more resistant to change.

g. This method requires knowledge of existing inlet conditions, assumed to be equilibrium conditions. Minimum data needed include a survey of the inlet throat cross section and the lag between high water in the ocean and the following slack water in the inlet. Czerniak (1977) found that the O'Brien and Dean stability theory was quite successful in explaining observed behavior at Moriches Inlet, New York. Interpretation of inlet history provided qualitative verification of the hydraulically unstable portion of the inlet hydraulic curve (Escoffier diagram) in both the scour and shoaling modes as well as semi-quantitative verification of the unstable scour mode. Results suggested that the theory could be applied to a broad range of inlet-related problems including those dealing with hydraulic design, sand bypassing design, control of bay tidal conditions, and effects of jetties on inlet stability.